Applied Energy 91 (2012) 51–58

Contents lists available at SciVerse ScienceDirect

Applied Energy

journal homepage: www.elsevier.com/locate/apenergy

Thermodynamic comparison of Peltier, Stirling, and vapor compression portable coolers

Christian J.L. Hermes [a,*], Jader R. Barbosa Jr. [b]

[a] Center for Applied Thermodynamics, Department of Mechanical Engineering, Federal University of Paraná, PO Box 19011, 81531990 Curitiba-PR, Brazil
[b] POLO Research Laboratories for Emerging Technologies in Cooling and Thermophysics, Department of Mechanical Engineering, Federal University of Santa Catarina, 88040900 Florianópolis-SC, Brazil

ARTICLE INFO

Article history:
Received 19 February 2011
Received in revised form 23 August 2011
Accepted 24 August 2011
Available online 5 October 2011

Keywords:
2nd Law efficiency
Peltier
Stirling
Vapor compression
Refrigeration
Performance comparison

ABSTRACT

The present study compares the thermodynamic performance of four small-capacity portable coolers that employ different cooling technologies: thermoelectric, Stirling, and vapor compression using two different compressors (reciprocating and linear). The refrigeration systems were experimentally evaluated in a climatized chamber with controlled temperature and humidity. Tests were carried out at two different ambient temperatures (21 and 32 °C) in order to obtain key performance parameters of the systems (e.g., power consumption, cooling capacity, internal air temperature, and the hot end and cold end temperatures). These performance parameters were compared using a thermodynamic approach that splits the overall 2nd law efficiency into two terms, namely, the internal and external efficiencies. In doing so, the internal irreversibilities (e.g., friction in the working fluid in the Stirling and vapor compression machines, Joule heating and heat conduction in the thermoelectric devices of the Peltier cooler) were separated from the heat exchanger losses (external irreversibilities), allowing the comparison between different refrigeration technologies with respect to the same thermodynamic baseline.

1. Introduction

One of the major concerns regarding vapor compression refrigeration is their *direct* contribution to the greenhouse effect resulting from gas leakage or end-of-life disposal. Alternative cooling technologies that do not use HCFCs or HFCs are often regarded as less harmful to the environment. Nevertheless, in addition to its low first cost and high reliability, vapor compression cooling has a comparatively smaller *indirect* contribution to global warming than other existing electricity-driven refrigeration technologies. This is because compressors are generally quite efficient in converting electricity into fluid enthalpy and a great number of vapor compression systems do not require secondary loops (e.g., indirect expansion) to transfer energy to and from the thermal reservoirs. On the other hand, high noise levels associated with compressors can make vapor compression refrigeration less attractive for some particular noise-sensitive applications.

Review articles and reports on the benefits and limitations of conventional and alternative cooling technologies have been presented by a number of investigators. Gauger et al. [1] evaluated several alternative refrigeration technologies according to six technical assessment criteria (state-of-the-art, complexity, size and weight, maintenance, useful life and efficiency) with respect to their use in different refrigeration applications (domestic air conditioning, commercial air conditioning, mobile air conditioning, domestic refrigeration and commercial refrigeration). They concluded that none of the alternative refrigeration technologies were, at the time of their research, as attractive as adapting vapor compression refrigeration to non-CFC refrigerants. Similar conclusions have been drawn in a more recent review organized by Devotta and Sicars [2]. Tang et al. [3] also compared the main advantages and disadvantages of sorption and solid-state refrigeration technologies at low- and near-room temperature conditions. More recently, Tassou et al. [4] reviewed both current state of the art technologies and emerging cooling technologies with potential to reduce the environmental impact of refrigeration in the food industry. According to their study, the main barriers for a more widespread utilization of thermoelectric and Stirling cycle refrigeration are related to the lower efficiency and higher costs associated with these technologies in comparison with vapor compression refrigeration.

Despite the energy performance limitations and technical difficulties mentioned above, the need for substitute environmentally-friendly cooling technologies has motivated researchers and companies to develop alternative cooling systems for household refrigeration. The most significant advances in this front have been achieved in the field of thermoelectric cooling [5], where significant efforts have been directed to reducing the thermal resistance

* Corresponding author. Tel.: +55 41 3361 3239.
E-mail address: chermes@ufpr.br (C.J.L. Hermes).

0306-2619/$ - see front matter © 2011 Elsevier Ltd. All rights reserved.
doi:10.1016/j.apenergy.2011.08.043

Nomenclature

Roman

Q_c	heat transfer rate to the cold end, W
Q_h	heat transfer rate from the hot end, W
T_e	temperature of the external environment, K
T_c	temperature of the cold end, K
T_h	temperature of the hot end, K
T_i	temperature of the internal environment, K
UA	cabinet thermal conductance, W/K
W	power consumption, W
S_g	entropy generation rate, W/K
N_S	dimensionless entropy generation

Greek

ε_c	ideal (Carnot) coefficient of performance
ε_{ii}	internally ideal coefficient of performance
ε_s	actual coefficient of performance
η_e	external thermodynamic efficiency
η_i	internal thermodynamic efficiency
η_s	overall thermodynamic efficiency

between the heat transfer[1] media in the hot and cold environments (generally air) and the thermoelectric material [6]. In addition to the more common configuration of forced convection of air on bonded aluminum fin heat sinks, alternative options involving the following approaches have been proposed:

(i) liquid coolant forced flow on both sides of the thermoelectric modules to improve thermal conductance [7];
(ii) replacement of finned surface heat sinks on the cold side by encapsulated phase change material heat sinks to maintain a constant temperature and improve the cooling storage capability of the refrigerator [8];
(iii) the use of a thermosyphon (to act as a thermal diode) between the phase change material and the cold junction of the thermoelectric module to prevent heat leakage into the refrigerated compartment during power-off periods [9];
(iv) the use of thermosyphons assisted by capillary lift, forced or natural convection on the hot and cold sides of thermoelectric devices to improve heat dissipation to the ambient air [10,11].

Hybrid refrigerators (vapor compression–thermoelectric) were proposed by Vián and Astrain [12], who evaluated the performance of a refrigerator equipped with an intermediate temperature (0 °C) compartment, maintained by a thermoelectric module, that was less affected by temperature transients (compressor on–off). Rodríguez et al. [13] advanced an experimentally-validated computational model for simulating the behavior of a vapor compression refrigerator with a thermoelectric ice-maker.

Berchowitz and co-workers have worked extensively on the development of free-piston Stirling coolers for a diverse number of applications, including domestic refrigeration [14] and portable cooler boxes [15,16]. Berchowitz et al. [16] evaluated experimentally the performance of a 40-W cooling capacity Stirling cooler (40-l cabinet). Carbon dioxide thermosyphons were employed to minimize thermal resistances between the cold surface of the free-piston device and the cold air. Oguz and Ozkadi [17] integrated a free-piston Stirling cooler into a domestic refrigerator cabinet. A closed loop thermosyphon using R-134a was used on the cold side. Heat rejection from the hot heat to the external ambient was achieved via forced convection of air. Power consumption and temperatures (cold head, evaporation and cabinet) were evaluated as a function of refrigerant charge and applied voltage. More recently, Sun et al. [18] developed a V-type integral Stirling refrigerator that is applicable to domestic refrigeration (design cold-end temperature of 238 K). Peak cooling capacities of the order of 50 and 80 W were achieved with N_2 and He as the working fluids, respectively.

[1] For sake of brevity, the energy transfer due to heat interaction will be referred in this work simply as heat transfer.

Although the interest in alternative cooling technologies has grown in recent years, the number of papers specifically dedicated to *comparing* the thermodynamic performances of small cooling capacity refrigerators is still rather small. This number becomes more limited when one is concerned with portable systems like the cooler boxes evaluated in the present paper. Bansal and Martin [19] compared three small refrigerators (vapor compression, absorption and thermoelectric) of about 50-l capacity in terms of their energy efficiency, noise and overall cost. They carried out reverse heat load tests to determine the overall thermal conductance of the refrigerators' compartments (the vapor compression system had the poorest thermal insultation), and energy consumption tests with the refrigerators at 5 °C. Vapor compression was the most energy efficient (110 Wh/day, COP = 2.59) and cheaper, followed by thermoelectric (330 Wh/day, COP = 0.69) and absorption (410 Wh/day, COP = 0.47). However, the vapor compression system presented the highest noise (30.5 dB), compared with the quietest absorption unit (24.8 dB). More recently, Adeyanju [20] and Adeyanju et al. [21] compared the performances of thermoelectric and vapor compression refrigeration system, but their analysis was restricted to the amount of time needed to cool down a certain volume (0.325 l) of water by a specified temperature difference. As far as the present authors are aware, no systematic comparison of thermodynamic performances involving Stirling refrigerators has been done so far in the open literature.

The purpose of the present paper is to evaluate experimentally the performances of four portable coolers that employ three different refrigeration technologies (thermoelectric, free-piston Stirling and vapor compression), as seen in Table 1. The tests were conducted at two different ambient temperatures (21 and 32 °C) and aimed at determining key performance parameters of the systems (e.g., power consumption, cooling capacity, cabinet air temperature, etc.).

When comparing different technologies, it is important to respect the same ideal cycle baseline. This can be achieved by writing the overall 2nd-law efficiency as the product of internal and external efficiencies. While the former accounts for fluid friction and thermal gradients in the cycle components, the latter is related to the transfer of heat with a finite temperature difference between the cycle and the hot and cold reservoirs. As will be seen, such an analysis helps to elucidate the processes that contribute the most to lowering the overall efficiency in each technology, thus serving as a guideline for possible future improvements in each system.

2. Brief technology description

2.1. Peltier cooling

Thermoelectric cooling is a solid-state technology, whereby an electric voltage creates a temperature difference in a pair of dissimilar materials. A typical thermoelectric module is manufactured

Table 1
Characteristics of the cooling systems under analysis.

Characteristics	Thermoelectric	Stirling	Recip. compressor	Linear compressor
Cabinet volume (l)	56	26	31	34
Refrigerant	Electrons	Helium	HFC-134a	HFC-134a
Cold end heat exchanger	Air source, forced	Thermosyphon	Roll-bond, natural	Roll-bond, natural
Hot end heat exchanger	Air source, forced	Air source, forced	Air source, forced	Air source, forced
Voltage supply	120 VAC	12 VDC	24 VDC	12 VDC
Temperature control	Continuous	Continuous	On–off	On–off

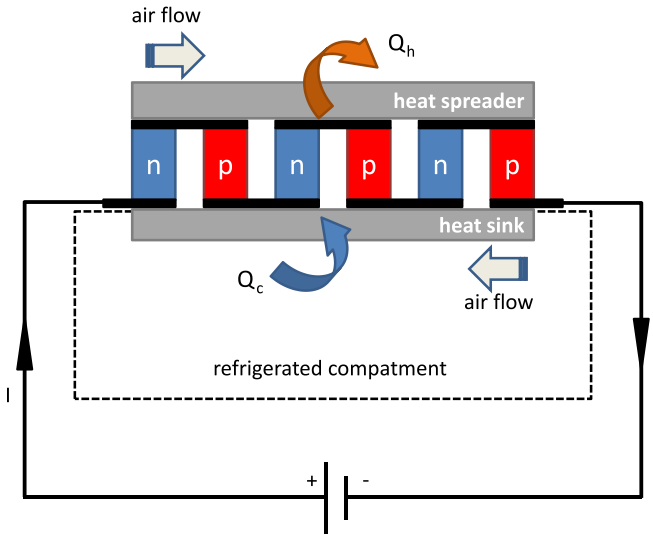

Fig. 1. Schematic diagram of a thermoelectric refrigerator with forced convection of air on the heat spreader (hot side) and on the heat sink (cold side).

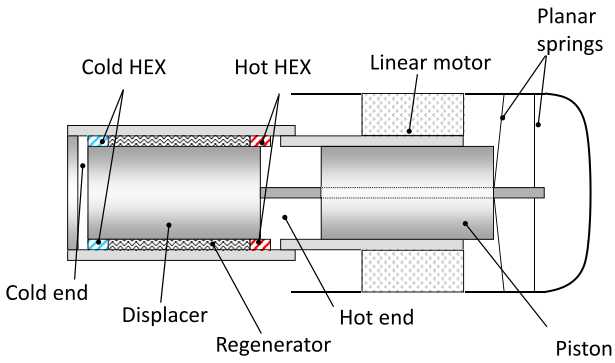

Fig. 2. Schematic representation of the internal components of the free-piston Stirling cooler.

with two thin ceramic wafers and an array of p- and n-type blocks of doped semiconductor material (e.g., bismuth-telluride) sandwiched between them (see Fig. 1). The n-type blocks have an excess of electrons, while the p-type blocks have a shortage of electrons. A pair of p- and n-type blocks connected electrically in series and thermally in parallel make up a thermoelectric couple. A thermoelectric module can contain up to several hundred thermoelectric couples. As electrons move from p to n through an electrical connector, they jump to a higher energy state and absorb energy from the surroundings (cold side). The opposite happens as they move from n to p, where the drop to a lower energy state causes an energy release to the surroundings (hot side). By inverting the polarity of the current, the direction of the heat transfer changes, as the cold side becomes the hot side and vice versa.

The thermal efficiency of a thermoelectric device can be related to the so-called dimensionless figure of merit, *ZT*, which is directly proportional to the electrical conductivity and to the Seebeck coefficient of the materials in the thermoelectric couple and inversely proportional to the thermal conductivity. Despite its low efficiency – the view is that *ZT* should be increased from the typical value of the order of unity to 3–4 in order to be competitive with vapor compression [1] – thermoelectric cooling has vast commercial applications due to its absence of moving parts and low noise.

2.2. Stirling cooling

Stirling coolers are based on an idealized gas cycle composed of two isochoric and two isothermal processes. In any of its many available configurations (α, β, γ), a system of pistons and displacers is used to move the working fluid – commonly air, H_2 or He – between volume spaces with a regenerator for thermal energy storage between steps of the cycle. In free-piston type machines, the pistons and displacers are not mechanically connected to a crankshaft, but supported by gas or planar springs [4], as shown in Fig. 2. The cooling capacity is determined by the piston amplitude, which is proportional to the voltage applied to the linear motor. Internal losses are minimized by using the high pressure working fluid as a gas bearing between the piston and the cylinder wall. In the cooler investigated in this paper, a passive secondary loop (thermosyphon) is attached to the cold end of the cooler to allow heat to be transferred from the cabinet. Heat rejection to the external environment is achieved by fan-assisted cooling of the hot end.

The thermodynamic processes occurring in the ideal cycle associated with the free-piston Stirling cooler are presented in Fig. 3. In process 1–2, the piston expands the working fluid in the hot end and heat is transferred to the system at constant temperature. Next, in 2–3, the displacer and piston move so as to maintain a constant volume. Energy is transferred to the regenerator. For this heat transfer process to be reversible, the temperature difference between the gas and the regenerator should not be larger than a differential amount *dT* at any point. Thus, a temperature gradient is created along the regenerator length. In process 3–4, the piston compresses the gas and heat rejection to the external ambient takes place at the hot heat exchanger. The temperature remains constant. Finally, in 4–1, the displacer and piston move (constant volume), and energy is transferred from the regenerator. A reversible heat transfer process occurs in the idealized Stirling cooling cycle.

2.3. Vapor compression cooling

In the vapor compression cycle, a volatile fluid (refrigerant) evaporates at approximately constant pressure as it extracts energy from the cabinet air. After leaving the evaporator, it enters the compressor where it is compressed up to the condensing pressure. In the condenser, the high-temperature gas rejects energy to the environment at approximately constant pressure. After condensation, the refrigerant is throttled in a capillary tube (or other

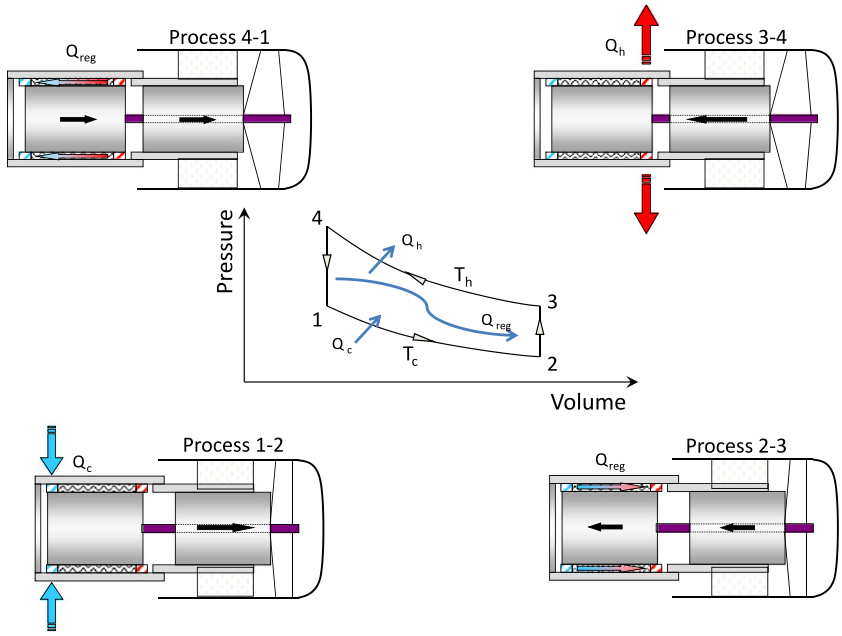

Fig. 3. The four thermodynamic processes in the idealized Stirling cooling cycle.

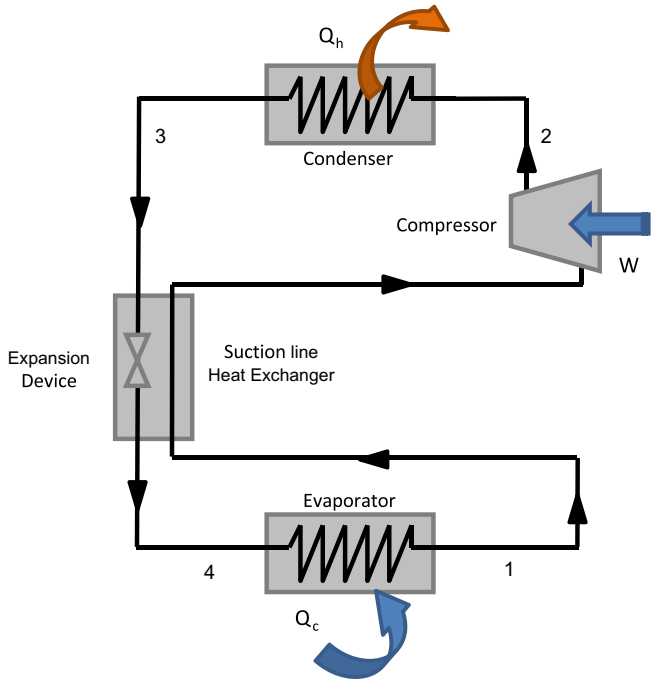

Fig. 4. The components of the vapor compression cooling cycle.

type of expansion device), thereby reducing its temperature and pressure down to the evaporating pressure. A schematic diagram of the vapor compression cooling system is shown in Fig. 4.

In some systems, a suction line heat exchanger is used, where the refrigerant exiting the evaporator exchanges heat with that flowing through the capillary tube. This ensures that the refrigerant is superheated before entering the compressor at the same time as it reduces the quality of the two-phase refrigerant entering the evaporator, thus contributing to improving its refrigerating effect.

3. Comparison methodology

The coefficient of performance of a real refrigeration system, ε_s, is defined as the ratio between the cooling capacity and the power consumption, as follows:

$$\varepsilon_s = Q_c/W \tag{1}$$

where $Q_c = UA(T_e - T_i)$ at steady-state, and UA is the thermal conductance of the refrigerated compartment (W/K). For an ideal refrigerator, the coefficient of performance depends only on the temperatures of the internal, T_i, and external, T_e, environments (see Fig. 5), being calculated from:

$$\varepsilon_c = T_i/(T_e - T_i) \tag{2}$$

If one assumes that the cooling device operates ideally between the cold, T_c, and hot, T_h, ends (see Fig. 5), the coefficient of performance considering the thermal losses due to the external irreversibilities (i.e., heat transfer with finite temperature difference in the heat exchangers) is calculated from:

$$\varepsilon_{ii} = T_c/(T_h - T_c) = (T_i - \Delta T_c)/(T_e - T_i + \Delta T_h + \Delta T_c) \tag{3}$$

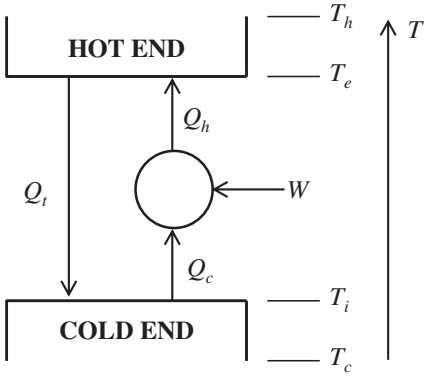

Fig. 5. Thermodynamic representation of a cooling system.

It should be noted that ε_{ii} is the maximum coefficient of performance possible for the cooling device if heat transfer across finite temperature differences is allowed to occur in the heat exchangers. In other words, ε_{ii} is the coefficient of performance of an ideal cooling device operating with real heat exchangers (the index *ii* stands for *internally ideal*).

The 2nd law efficiency associated with the internal irreversibilities (thermodynamic losses in the cooling device) can be calculated comparing the coefficient of performance of the real refrigeration system, ε_s, with that obtained assuming an ideal cooling device with real heat exchangers, ε_{ii}, as follows:

$$\eta_i = \varepsilon_s/\varepsilon_{ii} \tag{4}$$

Similarly, the 2nd law efficiency associated with the external irreversibilities (thermodynamic losses due to heat transfer across finite temperature difference in the heat exchangers) is calculated from:

$$\eta_e = \varepsilon_{ii}/\varepsilon_c \tag{5}$$

Therefore, the overall 2nd law efficiency of the entire refrigeration system is given by:

$$\eta_s = \varepsilon_s/\varepsilon_c = (\varepsilon_s/\varepsilon_{ii})(\varepsilon_{ii}/\varepsilon_c) = \eta_i\eta_e \tag{6}$$

Furthermore, the rate of entropy generation due to the thermodynamic losses in the cooling device can be calculated from the following entropy balance considering the temperatures of the cold, T_c, and hot, T_h, ends as references [22]:

$$S_g = W/T_h + Q_c(1/T_h - 1/T_c) \tag{7}$$

where S_g is the rate of entropy generation in the cooling device (W/K). The dimensionless entropy generation rate (a.k.a. the entropy generation number), N_S, is calculated from:

$$N_S = T_c S_g/Q_c \tag{8}$$

Based on Eqs. 1, 7, and 8, it can be shown that the system coefficient of performance can be expressed as:

$$\varepsilon_s = (T_i - \Delta T_c)/(T_e - T_i + \Delta T_h + \Delta T_c + T_h N_S) \tag{9}$$

In Eq. (9), that the term $T_h N_S$ is an equivalent temperature difference that accounts for irreversibilities taking place in the cooling device (i.e., internal losses). It should be noted that $\varepsilon_s \to \varepsilon_{ii}$ as $N_S \to 0$, and $\varepsilon_s \to \varepsilon_c$ as both ΔT_c and ΔT_h tend to zero. In other words, the temperature differences in the hot and cold ends of the cooling device and the inner boundary entropy generation rate cause a deviation between ε_s and its ideal counterpart, ε_c, thus reducing the system efficiency.

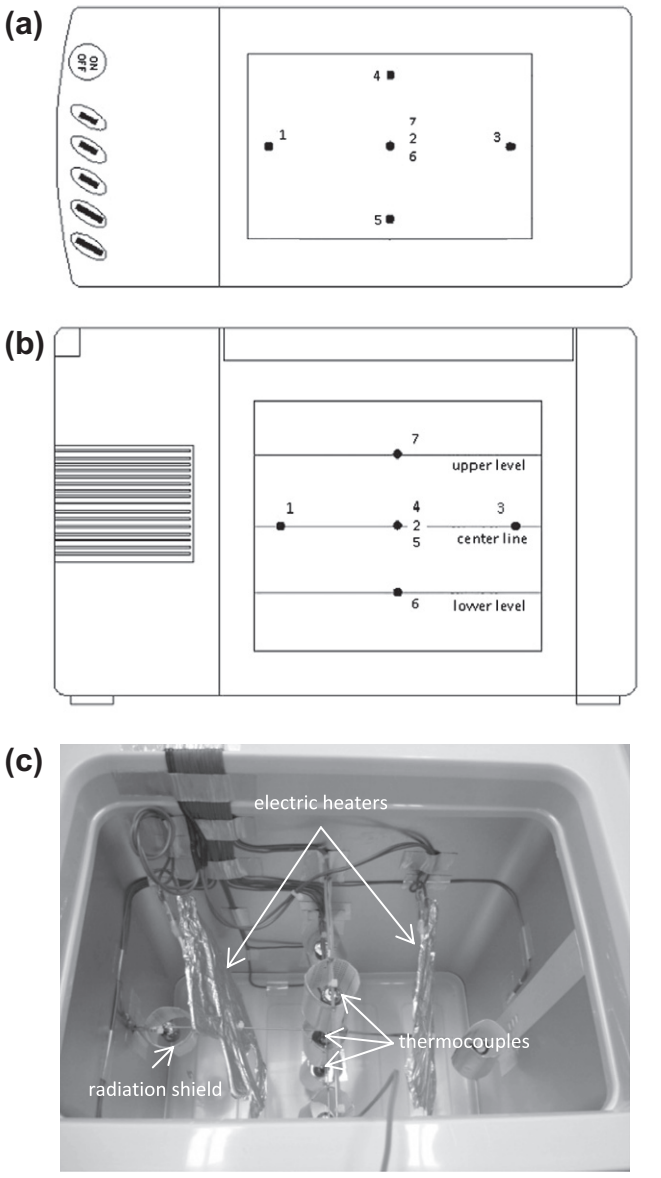

Fig. 6. Schematic of the cabinet air instrumentation with thermocouples: (a) top view, (b) side view (Stirling cooler) and (c) photography.

4. Experimental work

The experimental work described in this section refers only to the Stirling and vapor compression coolers. The thermoelectric cooler data were obtained from Duarte [23], who carried out a performance evaluation of the thermoelectric cooler described in Table 1 using experimental facilities and techniques equivalent to those employed in the present work for testing the Stirling and vapor compression refrigeration systems.

4.1. Temperature and power measurements

The coolers were tested in a climatized chamber, with a strict control of the air temperature, humidity and velocity. The cabinet air temperature and the temperature of several points on the refrigeration system were measured using T-type thermocouples with a measurement uncertainty of ±0.2 °C. The thermocouples used for measuring the cabinet air temperatures were brazed in cylindrical copper blocks, according to the recommendation of the ISO/FDIS standard 15502 [24]. The blocks act as thermal filters that reduce the high frequency, low amplitude temperature oscillations typical of the turbulent air flow. The average cabinet air temperature was obtained from seven thermocouples, five of which were positioned at the horizontal mid-plane of the cabinet. The remaining two were placed at the central vertical axis, as depicted in Fig. 6.

The surrounding air temperature was measured at three different positions around the coolers (front, right and back sides). For the thermoelectric and Stirling refrigerators, the hot and cold end temperatures were measured using surface thermocouples placed in between the hot and cold heads and the heat exchangers. For the vapor compression coolers, the thermocouples were placed on the refrigerant tubing along the heat exchangers so that the condensing and evaporating temperatures could be determined. All the surface thermocouples employed a thin electrical insulation media between the thermocouple and the tube fittings in order to avoid undesired electrical biasing. The power consumption of the cooling system was measured using a digital power analyzer with a mea-

Table 2
Summary of cabinet identification tests.

Refrigeration system	Thermoelectric		Stirling		Recip. compressor		Linear compressor	
Ambient temperature (°C)	21.4	31.5	21.0	21.0	21.1	21.2	21.0	21.0
Cabinet air temperature (°C)	46.2	56.7	45.0	54.9	44.7	54.2	44.8	54.9
Temperature difference (°C)	24.8	25.2	24.0	33.9	23.6	33.0	23.8	33.9
Fan power (W)	1.6	1.6	0.0	0.0	0.0	0.0	0.0	0.0
Internal power dissipation (W)	13.4	14.8	11.3	16.6	11.3	16.3	9.1	13.3
Cabinet *UA* (W/K)	0.60	0.65	0.47	0.49	0.48	0.49	0.38	0.39
Average *UA* (W/K)	0.63		0.48		0.49		0.39	

surement uncertainty of ±0.1%. The compression power was monitored during the refrigerator tests, whereas the power consumption of the other components (i.e., evaporator and condenser fans, control board) was measured *a priori*, i.e., before testing the refrigerator. Maximum propagated measurement errors of ±1 W and ±0.05 W/K were achieved for the cooling capacity and the cabinet conductance (*UA*), respectively, whereas maximum measurement errors of ±0.1 and ±0.01 were calculated for ε and η, respectively.

4.2. Cabinet UA identification

Before comparing the different refrigerating appliances, it is fundamental to determine the thermal load imposed on each cooler. This can be achieved by calculating the thermal conductance (*UA*) of the refrigerated compartment. In this study, the thermal conductances were calculated based on the reverse heat leakage approach [25], whereby the indoor temperatures are kept higher than the surrounding temperature due to heat dissipation within the refrigerated compartment through electric heaters. During the test, the refrigeration system is switched off and the cabinet and surrounding temperatures and the power dissipated by the electric heaters (W_i) at steady-state are monitored. If applicable, the evaporator fan must be switched on (W_f) to homogenize the compartment temperature (T_i) and to provide the actual convection on the cabinet walls. The thermal conductance is calculated from an energy balance as follows:

$$UA = (W_i + W_f)/(T_i - T_e) \quad (10)$$

Two tests were performed for each refrigeration system under two different conditions, as shown in Table 2, which also summarizes the resulting *UA* values for each refrigeration system under analysis.

4.3. Test planning and results

The coolers were tested at two different ambient temperatures (21 and 32 °C) at their maximum cooling capacities, so that a steady-state condition could be reached in all cases. The raw data for the ambient, cabinet air, cold and hot ends temperatures and also for the power consumption and cooling capacity are summarized in Table 3.

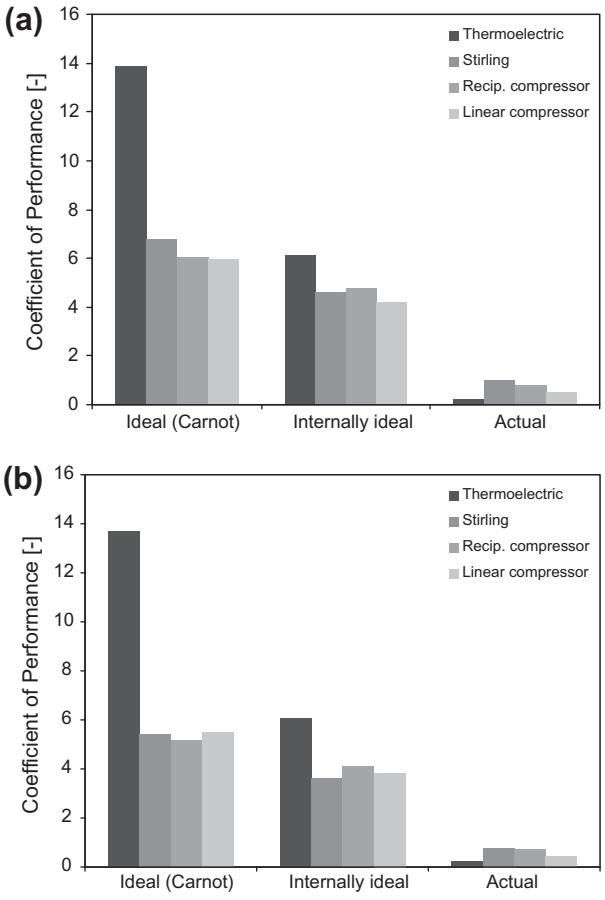

Fig. 7. Coefficient of performance: ambient air at (a) 21 °C and (b) 32 °C.

5. Discussion

Fig. 7 compares the actual, internally ideal and ideal coefficients of performance for the four refrigeration systems under analysis for ambient temperatures of 21 and 32 °C. It can be seen that, for an ambient air at 21 °C, the thermoelectric cooler showed the lowest ε_s (~0.2) followed by the vapor compression system with the linear compressor (~0.5), the vapor compression system with the

Table 3
Summary of steady-state test results.

Refrigerator	Thermoelectric		Stirling		Recip. compressor		Linear compressor	
Ambient temperature (°C)	21.9	31.6	21.0	31.9	21.1	32.0	21.2	32.3
Cabinet air temperature (°C)	2.1	10.8	−16.8	−15.9	−20.5	−17.6	−21.0	−14.8
Cold end temperature (°C)	−4.3	4.9	−27.1	−28.8	−23.9	−21.7	−27.8	−22.4
Hot end temperature (°C)	39.6	50.7	26.6	39.3	28.2	39.3	30.3	43.3
Power consumption (W)	55.5	56.6	18.3	30.5	25.7	32.9	34.0	42.4
Cooling capacity (W)	12.5	13.1	18.1	23.0	20.4	24.3	21.2	32.3

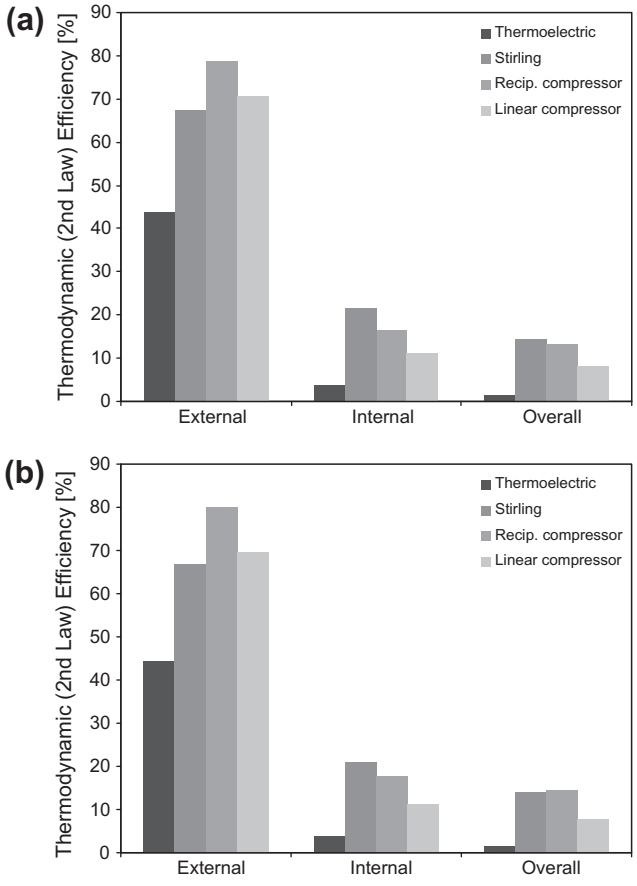

Fig. 8. Second law efficiency: ambient air at (a) 21 °C and (b) 32 °C.

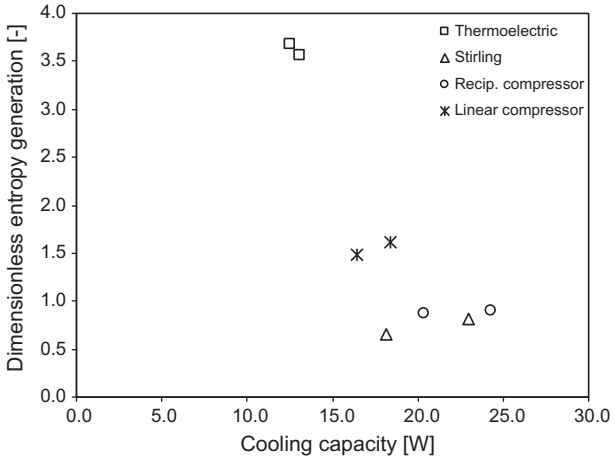

Fig. 9. Dimensionless entropy generation: ambient air at (a) 21 °C and (b) 32 °C.

reciprocating compressor and the Stirling cooler (~1.0). At 32 °C, the figures reduce slightly for all systems but the thermoelectric cooler. The ε_s reduction with the ambient temperature was more pronounced in the case of the Stirling cooler because its hot end temperature increased while the cold end temperature remained practically the same. This effect was not so intense for the two vapor compression systems since their cold end (evaporating) temperatures also changed. For the thermoelectric cooler, the influence of the ambient temperature on ε_s was practically of no significance, as both hot and cold end temperatures varied dramatically.

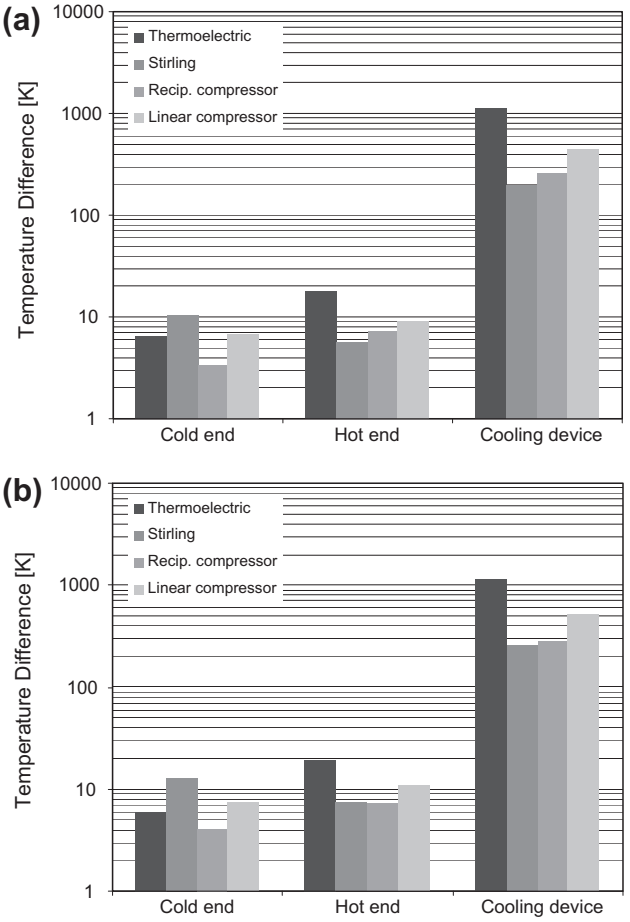

Fig. 10. Temperature differences in Eq. (9): ambient air at (a) 21 °C and (b) 32 °C.

Also in Fig. 7, it can be noted that the ideal (Carnot) coefficient of performance of the thermoelectric cooler was twice as high as those of the other systems because it generates the smallest temperature difference between the hot and cold environments. However, since the cooling capacity of the thermoelectric cooler was the smallest per unit input power, its overall thermodynamic efficiency was the lowest (~1%, i.e. a figure within the measurement uncertainty thresholds). On the other hand, the overall efficiencies of the Stirling and vapor compression coolers were around 10% (see Fig. 8). The small value of the internal efficiency of the thermoelectric cooler seen in Fig. 8 means that the internal irreversibilities in the thermoelectric module can be quite high. Indeed, this combined with the comparatively large value of its internally ideal coefficient of performance confirms the need for improvement of the thermoelectric properties of the thermoelectric cooler.

The Stirling device and the reciprocating vapor compression system presented the highest 2nd-law efficiencies (~14%), whereas the linear compressor system showed an overall efficiency of 8%. The good performance of the Stirling cooler was somehow expected due to its small rate of entropy generation (see Fig. 9) and high internal efficiency. On the other hand, the discrepancy between the performances of vapor compression systems was not. An observation of Figs. 7 and 8 reveals that the difference between the vapor compression systems performances is due to the effectiveness of their heat exchangers (see the internally ideal coefficient of performance in Fig. 7 and the external efficiency in Fig. 8) and to the performances of the refrigeration cycles (see the internal efficiency plotted in Fig. 8 and also the dimensionless entropy generation in Fig. 9).

It is also worthy of note that although the Stirling device presented the highest internal efficiency (see Fig. 8), its external efficiency (associated with the heat exchangers) is not as high as that obtained for the reciprocating vapor compression refrigeration system, which explains why both coolers have shown similar overall efficiencies. Another conclusion that can be drawn from Fig. 8 is that the external efficiencies of the direct expansion cooling systems (vapor compression) are higher than those calculated for the indirect expansion cooling systems (thermoelectric and Stirling), suggesting that the performance improvement of emerging cooling technologies also relies on the design of more efficient heat exchangers.

Fig. 9 shows the dimensionless (inner bound) entropy generation as a function of the cooling capacity for all refrigeration systems. The lowest dimensionless entropy generation rates are observed for the Stirling and reciprocating compressor refrigeration systems as they offer similar cooling capacities and also have similar internal efficiencies. The thermoelectric cooler showed the highest entropy generation number due to the low-efficiency cooling device. Fig. 10 complements the information presented in Figs. 7–9 by showing the temperature differences between the hot end and the external environment, the cold end and the cabinet air, and also the equivalent temperature difference associated with the internal entropy generation in the cooling device (i.e., the term $T_h N_S$ in Eq. (9)). It can be seen that the term $T_h N_S$ is nearly one order of magnitude higher than ΔT_c and ΔT_h showing that the internal irreversibilities play a major role in the system coefficient of performance.

6. Conclusions

A methodology for the thermodynamic comparison of different refrigeration systems based on different cooling technologies was outlined in this paper. A thermoelectric, a Stirling and two vapor compression refrigeration systems were tested at two different ambient temperatures (21 and 32 °C) using a climatized chamber. The operating parameters of the systems (power consumption, cooling capacity, internal air temperature, and the hot end and cold end temperatures) were used to derive thermodynamic performance parameters (coefficient of performance, 2nd law efficiency, dimensionless inner bound entropy generation rate) that were used to quantify the internal irreversibilities of the cooling devices (e.g., friction in the working fluid in the case of Stirling and vapor compression, Joule heating and heat conduction in the thermoelectric devices of the Peltier cooler) and also the external irreversibilities associated to heat transfer across finite temperature heat exchangers. The main conclusions of the study are as follows:

- The Stirling and the reciprocating vapor compression refrigeration systems presented similar overall thermodynamic efficiencies (∼14%), followed by the linear vapor compression system (∼8%) and then by the thermoelectric cooler (∼1%).
- Despite the fact that the Stirling cooler is more internally efficient than the reciprocating vapor compression cycle, the latter promotes a more efficient heat transfer between the cycle and the reservoirs due to its direct expansion heat exchangers. As a result, the overall efficiencies of the cycles were similar.
- The linear compression system presented lower internal and external efficiencies than its reciprocating counterpart, which is due not only to the heat exchangers thermal–hydraulic design (heat transfer area and fan characteristics) but also to the efficiency of the cycle itself.
- As far as the thermodynamic performance is concerned, the thermoelectric device is not at the same level as the other coolers. Serious improvement is needed to reduce both internal and external irreversibilities.

Acknowledgments

This study was carried out at the POLO Labs under National Grant No. 573581/2008-8 (National Institute of Science and Technology in Cooling and Thermophysics) funded by CNPq. Thanks are addressed to Messrs. L. van Bömmel, D.S. Oliveira and J. Purkote Neto for their valuable support with the experiments. The authors are grateful to Professor C. Melo (Federal University of Santa Catarina) and Mr. P.O.O. Duarte (presently at Whirlpool S.A.) for providing them with the thermoelectric cooler experimental data.

References

[1] Gauger DC, Shapiro HN, Pate MB. Alternative technologies for refrigeration and air-conditioning applications, United States environmental protection agency, Project Summary EPA/600/SR-95/066; 1995.
[2] Devotta S, Sicars S. Refrigeration. In: Safeguarding the ozone layer and the global climate system, special report of the intergovernmental panel on climate change, Cambridge University Press, UK; 2006. [Chapter 4]
[3] Tang C, Luo Q, Li X, Zhu X. Comparison of several eco-friendly refrigeration technologies. In: Proceedings of the sixth international conference for enhanced building operations, ICEBO2006, Shenzhen, China; November 6–9 2006.
[4] Tassou SA, Lewis JS, Ge YT, Hadawey A, Chaer I. A review of emerging technologies for food refrigeration applications. Appl Therm Eng 2010;30:263–76.
[5] Riffat SB, Ma X. Thermoelectrics: a review of present and potential applications. Appl Therm Eng 2003;23:913–35.
[6] Min Gao, Rowe DM. Experimental evaluation of prototype thermoelectric domestic-refrigerators. Appl Energy 2006;83:133–52.
[7] Davis M, Manners B, Clarke P. Design of a 126 litre refrigerator/freezer commercial prototype. In: 23rd international conference on thermoelectrics, Adelaide, Australia; July 25–29 2004.
[8] Riffat SB, Omer SA, Ma X. A novel thermoelectric refrigeration system employing heat pipes and a phase change material: an experimental investigation. Renew Energy 2001;23:313–23.
[9] Omer SA, Riffat SB, Ma X. Experimental investigation of a thermoelectric refrigeration system employing a phase change material integrated with thermal diode (thermosyphons). Appl Therm Eng 2001;21:1265–71.
[10] Astrain D, Vián JG, Domínguez M. Increase of COP in the thermoelectric refrigeration by the optimization of heat dissipation. Appl Therm Eng 2003;23:2183–200.
[11] Vián JG, Astrain D. Development of a thermoelectric refrigerator with two-phase thermosyphons and capillary lift. Appl Therm Eng 2009;29:1935–40.
[12] Vián JG, Astrain D. Development of a hybrid refrigerator combining thermoelectric and vapor compression technologies. Appl Therm Eng 2009;29:3319–27.
[13] Rodríguez A, Vián JG, Astrain D. Development and experimental validation of a computational model in order to simulate ice cube production in a thermoelectric ice-maker. Appl Therm Eng 2009;29:2961–9.
[14] Berchowitz DM, Unger R. Experimental performance of a free-piston Stirling cycle cooler for non-CFC domestic refrigeration applications. In: 18th International congress of refrigeration, Montreal, Canada, August 10–17 1991.
[15] Berchowitz DM. Stirling coolers for solar refrigerators. In: International appliance technical conference, West Lafayette, USA; 1996.
[16] Berchowitz DM, McEntee J, Welty S. Design and testing of a 40 W free-piston Stirling cycle cooling unit. In: 20th International congress of refrigeration, Sydney, Australia, September 19–24 1999.
[17] Oguz E, Ozkadi F. Experimental investigation of a Stirling cycle cooled domestic refrigerator. In: 9th International refrigeration and air conditioning conference at Purdue, West Lafayette, IN, Paper R-19-3; 2002.
[18] Sun L, Zhao Y, Li L, Shu P. Performance of a prototype Stirling domestic refrigerator. Appl Therm Eng 2009;29:210–5.
[19] Bansal PK, Martin A. Comparative study of vapor compression, thermoelectric and absorption refrigerators. Int J Energy Res 2000;24:93–107.
[20] Adeyanju AA. Experimental comparison of thermolelectric refrigeration and vapour power compression refrigeration. J Eng Appl Sci 2010;5:221–5.
[21] Adeyanju AA, Ekwue E, Compton W. Experimental and theoretical analysis of a beverage chiller. Res J Appl Sci 2010;5:195–203.
[22] Bejan A. Entropy generation through heat and fluid flow. New York, USA: Wiley; 1982.
[23] Duarte POO. Performance evaluation of a thermoelectric refrigerator (in Portuguese). MEng thesis, Federal University of Santa Catarina, Florianopolis SC, Brazil; 2003.
[24] ISO/FDIS 15502. Household refrigerating appliances – characteristics and test methods. International organization for standardization, Geneva, Switzerland; 2005.
[25] Vineyard EA, Therese KS, Kenneth EW, Kenneth WC. Superinsulation in refrigerators and freezers. ASHRAE Trans 1998;104(2):1126–34.